Indonesian Journal of Material Research
e-ISSN: 2987-1654
Vol. 1, No. 3, November 2023

Indonesian Journal of MATERIAL RESEARCH

Research Paper

Synthesis, Structure, and Hirshfeld Surface Analysis of tetrakis(N,N'-diethylthiourea)bis(isothiocyanato)nickel

Husni Wahyu Wijaya[1,2]*, Danar[1], Zainal Abiddin[1], I Wayan Dasna[1,2]

[1] *Department of Chemistry, State University of Malang (Universitas Negeri Malang), Jl. Semarang 5, Malang, Jawa Timur, 65145, Indonesia*
[2] *Centre of Advanced Material for Renewable Energy, State University of Malang (Universitas Negeri Malang), Jl. Semarang 5 Malang, Jawa Timur, 65145, Indonesia*
***Corresponding author**: husni.wahyu.fmipa@um.ac.id

Abstract
The complex compound tetrakis(N,N'-diethylthiourea)bis(isothiocyanato)nickel or $[Ni(detu)_4(NCS)_2]$ (denoted as UMCC-1) has been synthesized by reflux method in two different solvents namely acetone and methanol. This study aims to synthesize, characterize, and analyze the Hirshfeld Surface complex UMCC-1, which was obtained using the reflux method with the mole ratio of $NiCl_2$: detu: KSCN is 1:2:4. Single crystals UMCC-1 in acetone and methanol are dark green in color with melting points of 135-137°C and conductivity of 66.4-84.4 μS. The FTIR absorption band analysis of the two crystals is very similar, ν(C=S) detu 590 cm^{-1} and ν(C≡N) isothiocyanate 2119 cm^{-1}. The refinement of the crystal structure from the single crystal XRD data shows that the two dark green crystals are a molecular type that has a distorted octahedral geometry with the same crystal lattice, monoclinic crystal lattice, P21/c1 space group (no.14), crystal lattice parameter *a*= 11.112(3) Å, *b*= 17.249(5) Å, *c*= 9.647(3) Å, and β = 100.785(10). However, the complex produced in acetone solvent has better refinement quality than methanol concerning %R = 3.27 and %R = 4.55, respectively. The UMCC-1 crystal shows intermolecular hydrogen bonds N−H−−−S(isothiocyanato) and intramolecular hydrogen bonds N−H−−−S(detu) with Hirshfeld Surface analysis showing a significant contribution of H−−−H (69.5%) on crystal packing.

Keywords
Nickel Complex, Mixed Ligand, N,N'-diethylthiourea Ligand, Isothiocyanato Ligand, Hirshfeld Surface Analysis

Received: 10 September 2023, Accepted: 17 November 2023
https://doi.org/10.26554/ijmr.20231313

1. INTRODUCTION

Complex compounds based on detu ligands with transition metals have been successfully synthesized and published. The detu ligand can bind to transition metals through 2 donor atoms, S and N, which act as terminal or bridge ligands (Ahmad et al., 2017). Complexes $[ZnCl_2(detu)_2]$ and $[CoCl_2(detu)_2]$ have been synthesized using the reflux method with ethanol solvent (Ajibade et al., 2013). The resulting complex compounds form a tetrahedral geometry with coordination of the metal center ion through the S atom belonging to detu. Different studies have successfully synthesized transition metals with other thiourea-derived ligands, including $[Pd(dmtu)_2(L_2)_2]Cl_2$ (L= phosphite ligand) (Aziz et al., 2018), $[Pd(dmtu)_4]Cl_2$, $[Pd(metu)_4]Cl_2$ (Nadeem et al., 2009) and $[Cu(metu)_4]Br_2$ (Mufakkar et al., 2011). In general, the coordination of thiourea-derived ligands in successfully reported complex compounds forms the coordination of the central atom with the S atom belonging to the thiocyanate derivative. The complexes formed lead to ionic complexes with chloride and bromide atoms as counter ions by forming tetrahedral geometry.

Complexes with Ni(II) central ion are quite interesting to study because of their ability as antibacterial, anti-microbial (Ahghari et al., 2020), electrodes (Danchovski et al., 2022), lithium batteries (Al-Omair et al., 2017), supercapacitors (Alekseeva et al., 2017), catalytic reactions (Breitenfeld et al., 2012), and electrocatalytic reactions (Barma et al., 2022). In addition, Ni(II) center ion complexes also have varied geometries: square planar (Binzet et al., 2013), tetrahedral (Al-Hazmi and El-Metwally, 2017), trigonal bipyramidal (Craig et al., 2018), and distorted octahedral (Tanase et al., 2000). The potential of many nickel(II) complexes provides opportunities for further development. Complex compounds of nickel(II) chloride salts and detu ligands have been successfully synthesized by forming the structure $[Ni(detu)_4]Cl_2$ (Alfurayj et al., 2016). The resulting complex has a square planar geometry with a P21/*n* space group. The central atom of nickel(II) forms coordination with detu, which acts as a Lewis base through 4 S atoms, forming a coordination number of 4. The chloride ion in the complex does not bind directly to the central ion but acts as a counter-anion, which results in the complex being ionic (Bowmaker et al., 2009). The magnetic properties possessed by the complex compound form a paramagnetic with a melting point of 141.8°C. A different study successfully

reported a complex compound of nickel(II) with thiourea ligand. The synthesis was carried out by direct reaction method with a ratio of 1:4 crystallized to form needles with a light green color. The complex compound has the structure $[Ni(tu)_6](NO_3)_2$, which produces monoclinic crystals with a *C2/c* space group and octahedral geometry (Monim-ul Mehboob et al., 2010). The thiourea ligand acts as a Lewis base that donates electron pairs in forming coordination with the nickel center ion, which is a Lewis acid.

Thiocyanate (SCN^-) ligands have become a frequently discussed topic in complex compound research in recent years (Hannachi et al., 2019). The contribution of thiocyanate ligands in complexes provides various chemical and physical properties (Zhang et al., 2017). Some complex compounds of thiocyanate ligands with transition metal atom centers are $[Zn(NCS)_2(_3{-}NH_2py)_2]$ (Yufanyi et al., 2021), $Co(NCS)_2(_4{-}NH_2py)_2]$ (Sugiyama et al., 2015), and $Cd(\mu{-}SCN)_2(_4{-}NH_2py)_2$ (Banerjee et al., 2005). In nickel(II) metal complexes with thiocyanate ligands generally form distorted octahedral geometries such as $[Ni(_2{-}amp)_2(SCN)_2(H_2O)_2]H_2O$ (Tabatabaee and Saheli, 2011) and $[Ni(_4{-}amp)_2(SCN)_2(H_2O)_2]$ (Neumann et al., 2018) with a six coordination number. The formation of coordination complexes is based on the theory of "Hard soft acid base", where nickel(II) is a borderline acid that tends to bond more with the mid-N base than the soft S base (Galet et al., 2005).

Some complex compounds with thiourea and thiocyanate derivatives as ligands that were successfully synthesized include $[Cd(metu)_2(NCS)_2]n$ (Ahmad et al., 2017), $[Ni(metu)_2(NCS)_2]n$ (Asif et al., 2019), and $[Ni[SC(NHCH_2)_2]_2(SCN)_2]n$ (Nardelli et al., 1966). The $[Ni(metu)_2(NCS)_2]n$ complex has space group P-1 with distorted octahedral geometry in its polymer formation (Asif et al., 2019). Coordination of Ni(II) center atom with thiocyanate ligand through nitrogen atom with Ni-NCS bond, while coordination with methylthiourea (metu) ligand tends to form ligand bridge through S atom of metu. The $[Ni[SC(NHCH_2)_2]_2(SCN)_2]n$ complex shows differences in the coordination of bridge ligands (Nardelli et al., 1966). Thiocyanate bridges between the two central atoms of Ni(II) through Ni−S and Ni−N coordination in zigzag chains, while thiourea derivatives act as terminal ligands. In this report, we have prepared a new complex in acetone and methanol solvent, structure, and Hirshfeld surface analysis of the dark green crystal of UMCC-1. This new compounds were successfully synthesis using the reflux method under methanol solvents from their precursor with mol ratio Ni(II): detu: SCN^- i.e., 1:2:4, respectively.

2. EXPERIMENTAL SECTION

2.1 Materials

The materials used in this study include $NiCl_2{-}_6H_2O$ (Merck), KSCN (Merck), N,N'-diethylthiourea (Merck), methanol, acetone (Merck), and distilled water. All reactants were used without prior purification.

2.2 Methods

The synthesis procedure of UMCC-1 was modified from the Co-detu complex (Wahyuni et al., 2022) and using methanol solvent. The detu ligand (0.264 g, 2 mmol) was dissolved into 5 mL of methanol at room temperature. A solution of nickel(II) chloride hexahydrate (0.237 g; 1 mmol) in 5 mL of methanol was added slowly. The dark green solution was stirred for four hours under reflux, then KSCN solution (0.388 g; 4 mmol of KCN in 5 mL of methanol) was slowly added and continued for reflux until three hours. Crystallization was carried out by evaporation slowly in a refrigerator, and the dark green crystal of UMCC-1 was obtained after four weeks. The synthesis procedure of UMCC-1 with acetone solvent is the same as that of methanol solvent.

The sample was characterized using melting point meter (Fisher Scientific), conductometer (Eutech CyberScan 400), and FTIR (Shimadzu IRPrestige 21 on KBr pellets in the 4000-400 cm^{-1} range). Crystal structure data of UMCC-1 were gathered at 236 K using XRD single crystal Bruker, D8 Quest Diffractometer equipped with a CCD area detector, and Mo Kα source (λ = 0.71073 Å) monochromated by layered confocal mirrors. Data reduction and scaling were performed using Bruker APEX 4 suite, and absorption correction was performed using SADABS. SHELXT was used to solve the initial structure, revealing non-hydrogen atom's positions, which was refined using the SHELXL program on a ShelXle user interface. Anisotropic refinement was performed on non-hydrogen atoms. Hydrogen atoms were placed in the calculated positions using a riding model. The Hirshfeld Surface Analysis was conducted with CrystalExplorer 17.5 on crystal structures imported from the CIF file (Psycharis et al., 2021). Trophotometer and the absorbance value was recorded.

3. RESULTS AND DISCUSSION

3.1 Synthesis of UMCC-1

The synthesis between $NiCl_2{-}_6H_2O$ with mixed ligands of detu and thiocyanate was carried out with a stoichiometric ratio of 1:2:4 in methanol and acetone solution. The proposed formation and crystal of UMCC-1 are shown in Figure 1. The methanolic solution of detu was added to the nickel solution slowly and then heated under reflux for four hours. The methanolic solution of KSCN was put into that mixture and continued reflux for four hours. The final dark green solution was sluggishly evaporated at room temperature. It resulted in the dark green needle-shaped crystals with 73.7% and 86.1% yield after two couple-weeks from methanol and acetone, respectively.

3.2 Structure of UMCC-1

The melting point test was initially carried out to justify that the formed crystal was a new compound by comparing it with the melting point of the precursors. The melting point measurements of UMCC-1 and their precursors are shown in Table 1. The UMCC-1 has different melting points from their precursors, i.e., the melting point of UMCC-1 and its salt is 137°C and 144°C, respectively. These results also compare the color differences between the UMCC-1 and their salts.

The electrical conductivity test of UMCC-1 was conducted to identify the complex dissociation in the solution as ionic or molecular. The conductivity of UMCC-1 in methanol gave a value of 84.5 μS, which was lower than their salts, i.e., nickel(II)

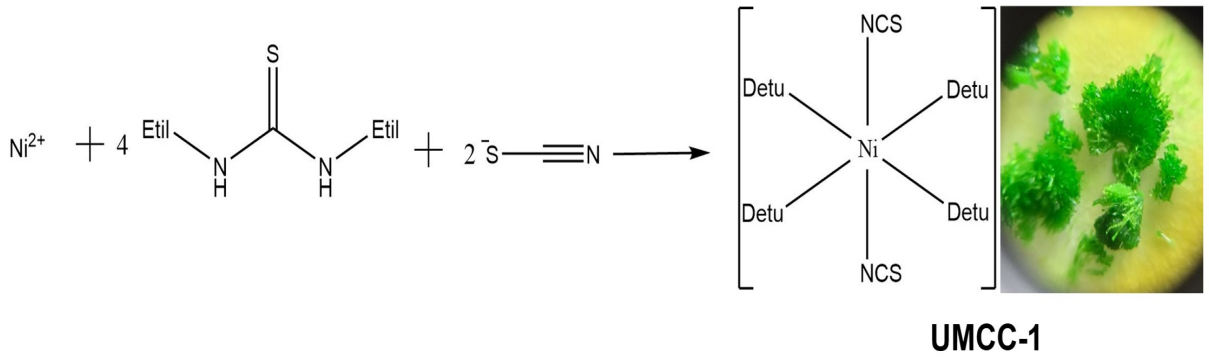

Figure 1. Proposed Reaction Formation of UMCC-1

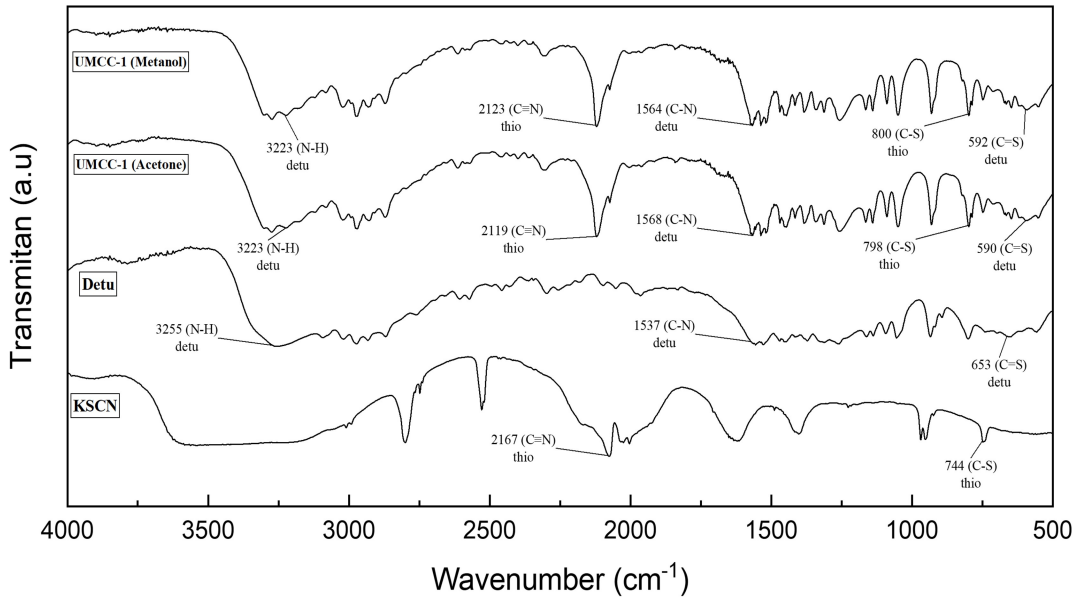

Figure 2. FTIR Spectrum of UMCC-1 and its Precursor

Table 1. Melting Point of UMCC-1 and its Precursor

Compounds	Melting point (°C)
UMCC-1	137 (methanol) 135 (acetone)
$NiCl_2$•$6H_2O$	144
Detu	68-71
KSCN	173

Table 2. Conductivity test UMCC-1 and its precursor in methanol

Compounds	Conductivity (μS) in 1.0 mg/mL
UMCC-1	84.5 (methanol) 66.4 (acetone)
$NiCl_2$	404
Detu	3.14
KSCN	832
Methanol	1.76

chloride and KSCN, as tabulated in Table 2. The result showed that UMCC-1 tended to be molecular in solution and in line with the suggestion of the melting point test result.

The functional groups of detu and thiocyanate as ligands were analyzed from FTIR, as shown in Figure 2. The absorption band of detu displays typical peaks at 3255 cm^{-1}, 1537 cm^{-1} and 653 cm^{-1}. However, ν(N—H) bond vibrations of detu as a ligand in the UMCC-1 appeared at wavenumber 3223 cm^{-1} (Table 3)

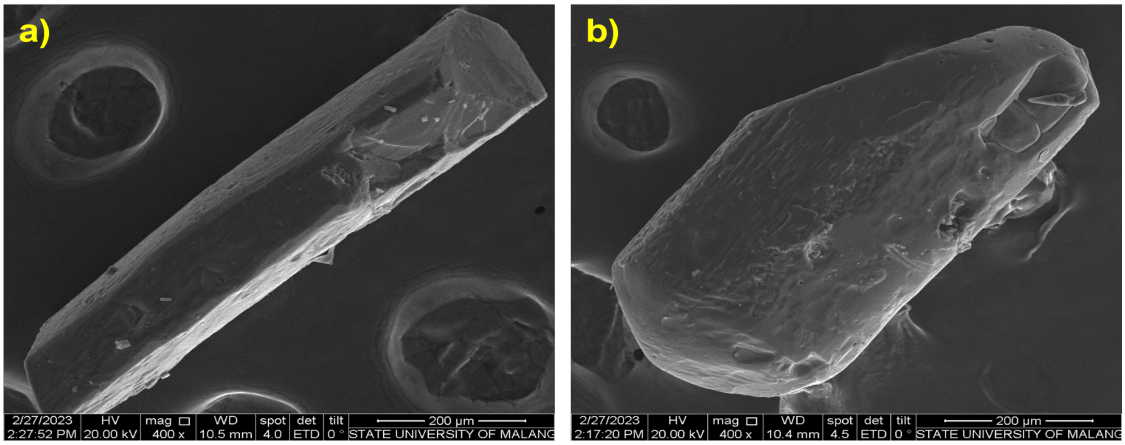

Figure 3. SEM Image at 400 Magnification of UMCC-1 Using Methanol (a) and Acetone (b)

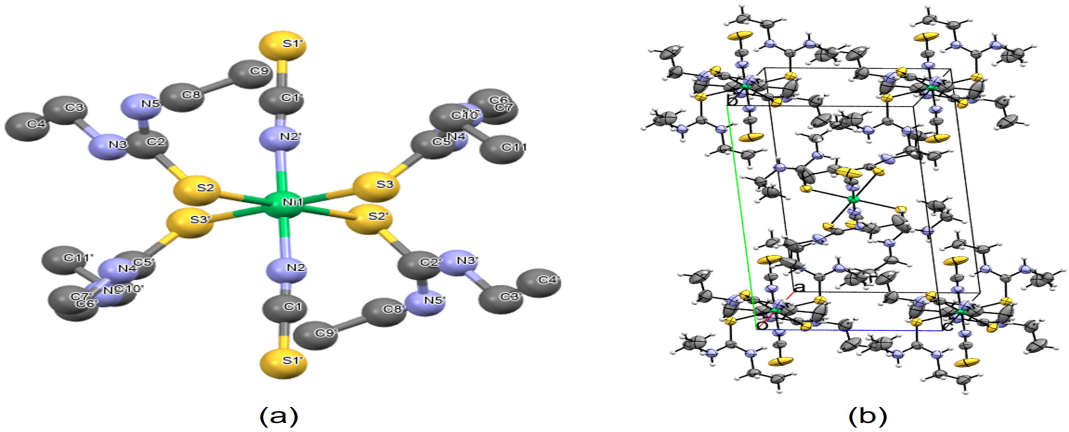

Figure 4. Structure of UMCC-1 (a) and its Crystal Lattice Packing (b)

and shifting of ν(N-H) vibration indicated the presence of hydrogen bonds between molecules when coordinating complex compounds (Ahmad et al., 2012). A significant wavenumber shift occurs in the ν(C−N) vibration, which indicates the involvement of detu in coordination with the central atom to form a coordination compound. While the ν(C=S) band shifted from 653 to 592 cm^{-1}, indicating the binding of the central atom with the S atom of thiocyanate, and the asymmetric C≡N stretching vibration shifted from 2167 to 2121 cm^{-1}, which predicted Ni-NCS coordination (Table 3). Another peak in the compound formed appeared vibrations at 2072 cm^{-1} absorption, which corroborates the formation of Ni−NCS coordination referring to the $[Ni(methu)_2(NCS)_2]n$ complex (Asif et al., 2019). This significant shift shows that the thiocyanato ligand is coordinated on nickel through the N atom (Tsague Chimaine et al., 2016).

The morphology of UMCC-1 was analyzed using scanning electron microscopy (SEM) at 400 magnifications, as shown in Figure 3. The SEM image confirms the rod-shaped single crystals of UMCC-1.

The chemical formula, structure analysis, coordination pattern, and bonding environment of UMCC-1 were determined from XRD-Single Crystal and its crystallographic data was tabulated in Table 4. UMCC-1 with acetone solvent has better refinement quality referring to the small %R-factor value than methanol, i.e., 3.27% and 4.55%, respectively. The structural information of UMCC-1 shows a coordination bond between the Ni(II) center ion with four S atoms derived from the detu ligand and two N atoms derived from the isothiocyanato ligand. This complex's Ni(II) central atom has six coordination numbers with

Table 3. FTIR Spectrum Interpretation of UMCC-1 and its Precursor

Vibration modes	Wavenumber (cm^{-1})		
	KSCN	detu	UMCC-1
ν(N−H)detu	-	3255	3223
ν(C−N)detu	-	1537	1564
ν(C=S)detu	-	653	592
ν(C−S)thio	744	-	800
ν(C≡N)thio	2167	-	2121

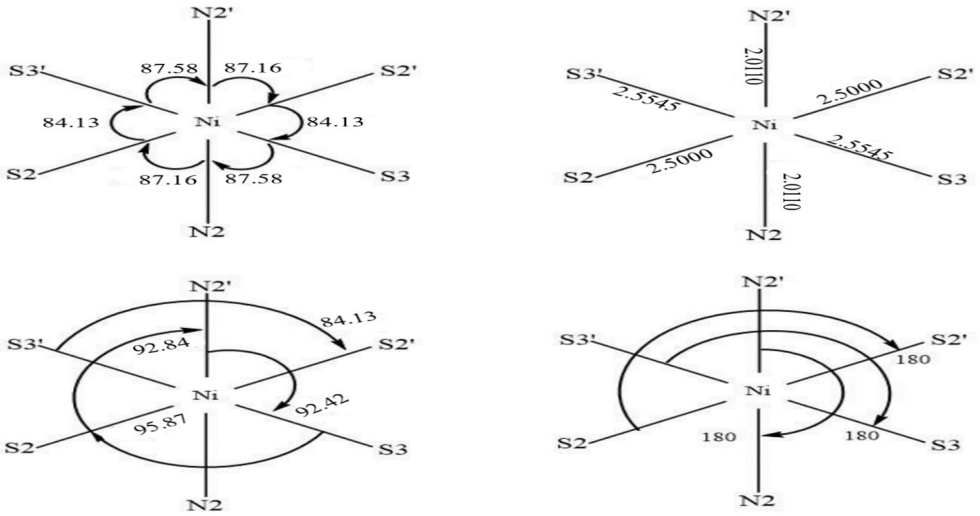

Figure 5. Schematic Core Geometry of UMCC-1

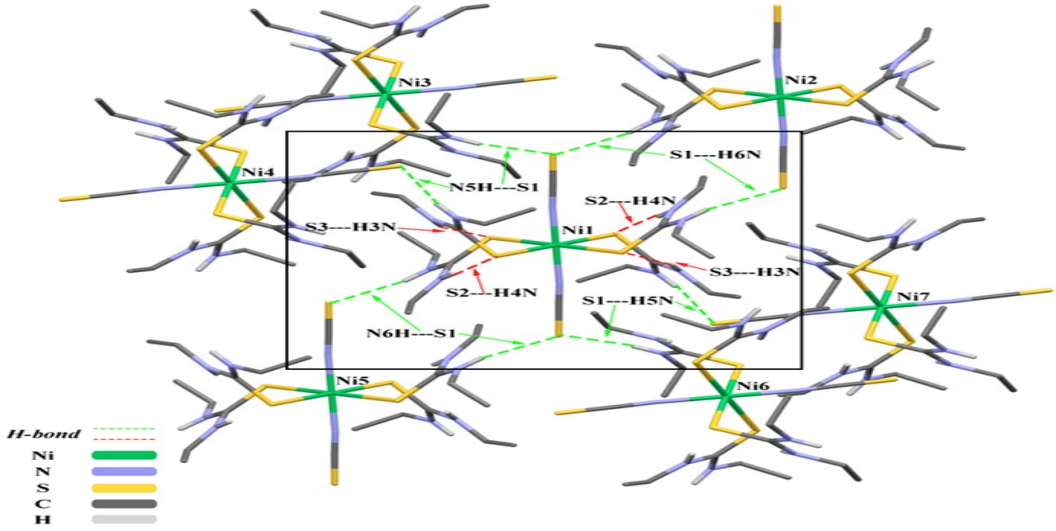

Figure 6. Schematic Intra- and Intermolecular Interaction of UMCC-1

distorted octahedral geometry, as shown in Figure 4. The isotiocyanato ligand in the complex structure coordinates with the Ni central atom through the donor atom N. This is in line with the "HSAB" theory, which states that the N atom (borderline base) tends to be attracted to Ni metal (borderline acid) compared to the donor atom S (soft base). In addition, the detu ligand and thiocyanato ligand only donate one donor atom, so they are referred to as monodentate ligands and do not act as bridge ligands.

The bond lengths and angles around the nickel center were presented in Table 5 and illustrated in Figure 5. The Ni-S bond is longer than the Ni−N bond, which is influenced by the steric hindrance of the detu, resulting in the elongation of the Ni−S bond. The N2−Ni−S2/S3 bond angle, which is below 90°, is also responsible for the elongation of the Ni−S bond. The repulsion of the N2−Ni−S2 (87.16°) and N2−Ni−S3 (87.16°) bond angles resulted in the Ni−S2/3 bond elongating to minimize the repulsion exerted by the nitrogen atom. The Ni−S bond lengths are comparable to those reported for $[Ni(metu)_2(NCS)_2]n$ (Asif et al., 2019), $[Ni(detu)_4]Cl_2$, and $[Ni(tu)_6](NO_3)_2$ (Monim-ul Mehboob et al., 2010) complexes ranging from 1.995(6)-2.572(13) Å. The bond length of Ni1−S3 is slightly higher than that of Ni1−S2. The bond difference of about 0.055 Å is possible because the S3 atom attracts more strongly C5 1.709(2) Å than S2−C2 1.723(2) Å (Table 7). Thus giving an elongation to the Ni1−S3 bond to minimize electron repulsion.

The shorter Ni-N bond provides information on strong binding between the central atom and the thiocyanato ligand. This is in line with the expectation that the binding of thiocyanato ligand is based on the "HSAB" theory. The nickel center atom

Table 4. Crystallographic Data of UMCC-1

Crystallographic data	UMCC-1
Chemical formula	$C_{22}H_{48}N_{10}NiS_6$
Molar mass	703.77 g/mol
Temperature	296 K
Wavelength	0.71073
Crystal System	Monoclinic
Space group	P21/c1 (no.14)
Lattice parameters	a= 11.1214(3) Å,
	b= 17.2492(5) Å,
	c= 9.6472(3) Å
	β = 100.785(10)
Volume	1816.48 (9)
R-Factor (%)	3.27
Z	2
Radiation	Mo-Kα
Theta max	28.280
$F(000)$	748.0
h,k,l_{max}	14,22,12
T_{min}, T_{max}	0.679, 0.746
R indices	R_1 = 0.0327
	wR_2 = 0.0785
CCDC number	2244641

Table 5. Bond Lengths and Bond Angles at Ni(II) Center Atoms

Bond lengths	(Å)	Bond Angles	(°)
Ni1–S2	2.5000(4)	S2–Ni1–S3	84.125(13)
Ni1–S3	2.5545(4)	S2–Ni1–N2	87.16(4)
Ni1–N2	2.0113(14)	S2–Ni1–S2'	180.00
		S2–Ni1–S3‘	95.875(14)
		S2–Ni1–N2‘	92.84(4)
		S3–Ni1–N2	87.58(4)
		S3‘–Ni1–S2	95.875(14)
		S3–Ni1–S3'	180.00
		S3–Ni1–N2‘	92.42(4)
		N2‘–Ni1–S2	92.84(4)
		N2‘–Ni1–S3	92.42(4)
		N2–Ni1–N2'	180.00
		S2‘–Ni1–S3‘	84.125(13)
		S2‘–Ni1–N2‘	87.16(4)
		S3‘–Ni1–N2 ‘	87.58(4)

Table 6. Bond Length and Bond Angle of Isothiocyanato Ligands

Bond length	(Å)	Bond angle	(°)
N2–C1	1.142(2)	N2–C1–S1	178.86(15)
C1–S1	1.6368(17)	Ni1–N2–C1	174.41(14)

belongs to mid acid, and the nitrogen atom belonging to thiocyanato is a mid-base, so the interaction is stronger than sulfur. In addition, nitrogen's electronegativity is higher than sulfur's, so nitrogen tends to have a greater bond energy. Consequently, the bond will be shorter, as evidenced by the Ni−S bond length, which is, on average, longer than Ni−N.

The bond lengths and angles of the thiocyanato ligands are shown in Table 6. The N−C bond is shorter than the C−S bond. This is due to the difference in bond order between N−C and C−S. The N−C bond order is higher so that the bond strength is stronger, as evidenced by the shortness of the bond. In comparison, the C−S bond order is less, which results in longer bonds than N−C and stabilizes the bond. The electronegativity of S, which is below the N atom, also contributes to the lengthening of the C−S bond.

The bond lengths and angles of the detu ligands are shown in Table 7. The average S−C bond is shorter than S−Ni. The shortening of bonds is due to the difference in bond order of S−C, which is higher than S−Ni. Thus, leading to shorten S−C bonds as a consequence of strong bonds. The bond angles of C2−N3/N5−C(ethyl) and C2−N4/N6−C(ethyl) ranged from 124.8(2) to 127.3(2)°. The bond angle, which is far below 180°, gives the amount of steric hindrance to the N atom of the detu ligand. It is also supported by the bulky structure of the ethyl functional group, which provides less space for the metal to covalently bond.

The steric effect of detu ligand on UMCC-1 gives an interesting effect for alkyl functional groups (Wada et al., 2004). The nickel and sulfur bond (detu) becomes longer with increasing size of alkyl on N atom. The magnitude of steric repulsion tu<metu<detu is proportional to the length of Ni-S bond tu<metu<detu due to alkyl addition. This was found in the studies of $[Ni(tu)_6](NO_3)_2$ (1.995(6) Å), $[Ni(detu)_4]Cl_2$ (2.230(2) Å), and $[Ni(metu)_2(NCS)_2]n$ (2.572(13) Å) complexes. However, increasing the distance Ni−S(methu) in the $[Ni(methu)_2(NCS)_2]n$ complex because methu acts as the bridge ligand. The steric effect of the functional group is also responsible for the elongation of the nickel(II) with N, which is proportional to the steric repulsion of the detu ligand.

Each molecule of UMCC-1 is directly connected with the other six molecules through N−H−−−S intermolecular bond of hydrogen-amine group with sulfur-isothiocyanato. The bonds of the six neighboring molecules are connected through a type of hydrogen bond with the same two S isothiocyanato and four amine groups. Other interactions are intramolecular complexes on each detu ligand through N−H−−−S detu. The types of intra- and inter-molecular hydrogen bonds are shown in Table 8 and simulated in Figure 6. In the crystal lattice, crystal packing of UMCC-1 is stabilized by intermolecular N−H−−−S interactions.

3.3 Hirshfeld surface analysis of UMCC-1

Hirshfeld surface analysis quantitatively measures and visualizes the interactions between molecules in the crystal. The strength of intermolecular interactions is visualized in the Hirshfeld surface using the d_{norm} description with Crystal-Explorer software

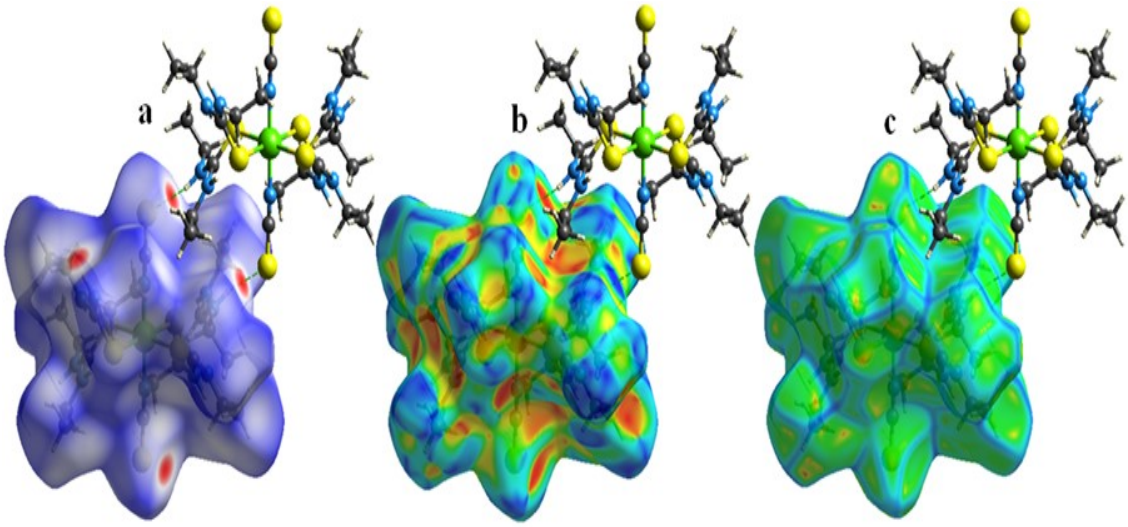

Figure 7. Hirshfeld Surface Plotted Over a) d_{norm} , b) Shape Index, and c) Curvedness of UMCC-1

Table 7. Bond Lengths and Bond Angles of Detu Ligand

Bond lengths	(Å)	Bond angles	(°)	Bond lengths	(Å)	Bond angles	(°)
S2−C2	1.723(2)	S2−C2−N3	120.2(1)	S3−C5	1.709(2)	S3−C5−NN	120.7(1)
C2−N5	1.325(2)	S2−C2−N5	121.2(1)	C5−N6	1.334(2)	S3−C5−N6	121.0(1)
C2−N3	1.327(2)	N3−C2−N5	118.5(2)	C5−N4	1.321(2)	N4−C5−N6	118.3(1)
N3−C3	1.454(2)	C2−N3−C3	125.6(2)	N4−C6	1.445(3)	C5−N4−C6	127.3(2)
N5−C8	1.453(2)	C2−N5−C8	125.2(2)	N6−C10	1.463(3)	C5−N6−C10	124.8(2)
C3−C4	1.506(3)	N3−C3−C4	110.2(2)	C6−C7	1.479(3)	N4−C6−C7	110.2(2)
C8−C9	1.496(3)	N5−C8−C9	111.7(2)	C10−C11	1.481(5)	N6−C10−C11	112.1(2)

Table 8. Intra- and Inter-Molecular Distance of UMCC-1

D–H−−A	D–H(Å)	H−−A(Å)	D–H−−A(Å)	(°)
N3–H3N−−S3	0.841(18)	2.539(18)	3.351(16)	162.80(17)
N4–H4N−−S2	0.860	2.470	3.319(16)	172.00
N5–H5N−−S1	0.847(16)	2.639(18)	3.393(17)	149.100(17)
N6–H6N−−S1	0.864(19)	2.630(2)	3.407(18)	150.200(17)

(Bhola et al., 2019). The calculation of the normalized contact distance (dnorm) is based on the contact distance of the nearest atom that is inside (d_i) to outside the surface (d_e) on a fixed color scale of 0.0870 (red) to 1.2944 (blue) au (Baydere et al., 2019). The red region around the S atom of the isothiocyanato and the deprotonated amine group indicates the presence of N−H−−−S hydrogen bond interactions in the crystal packing in Figure 7. The blue region indicates contact interactions with a positive dnorm value while the white color informs the contact distance equal to the Van der Waals radius (d_{norm} = 0) (Feddaoui et al., 2019).

The molecular shape index map measurements, as shown in Figure 7(b), produced red and blue regions representing hydrogen bond acceptors and donors, respectively (Ashfaq et al., 2021). The red spot near the S atom of isothiocyanato indicates interaction as a hydrogen bond acceptor. In contrast, a blue spot near the deprotonated amine group indicates the hydrogen bond donor. The results of the molecular curvature map show a green region representing a surface area that tends to be flat, while the blue region informs the curvature of the crystal (Azouzi et al., 2017).

The fingerprint plot pattern shows the significant contribution of intermolecular interactions to the Hirshfeld surface (Psycharis et al., 2021). The calculation of the 2D fingerprint plot is based on each interatomic contact and the overall interaction (Ashfaq et al., 2021). The distribution of H−−−H contact points is responsible for UMCC-1 crystal stability in the molecular fingerprint plot. The H−−−H interatomic contact

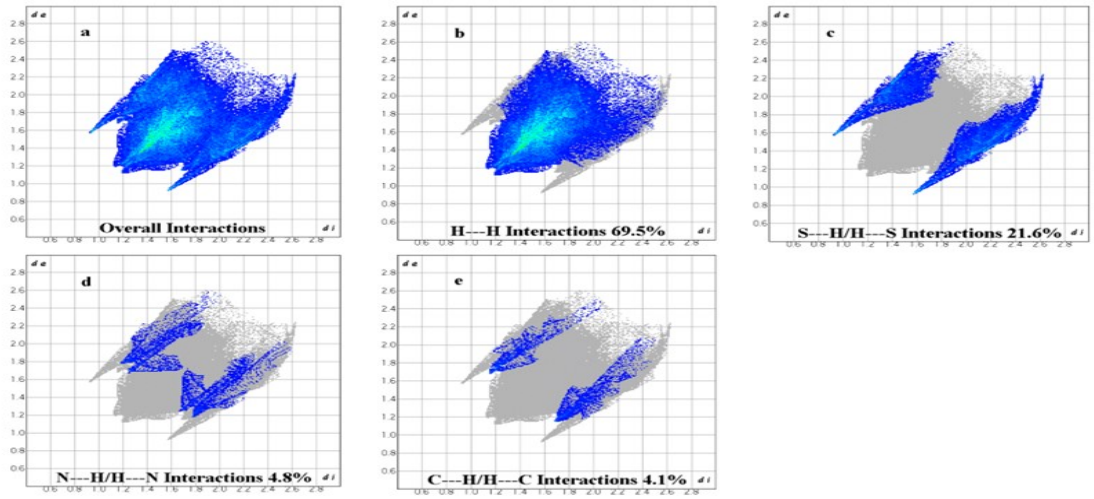

Figure 8. 2D Fingerprint Plots of Compound UMCC-1 Showing the Percentage Contacts of H−−−H, S−−−H/H−−−S, N−−−H/H−−−N, and C−−−H/H−−−C on the Total Hirshfeld Surface

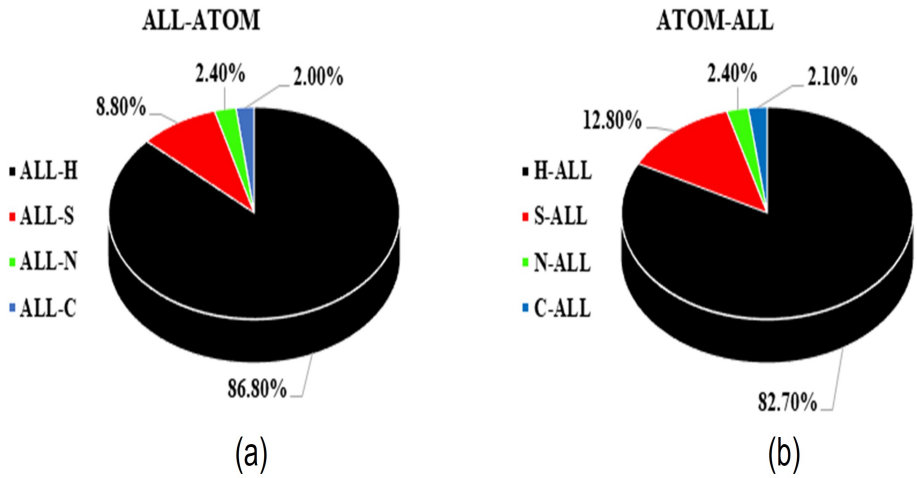

Figure 9. Percentage Contribution of Interactions (a) All Atoms to Atoms and (b) Atoms to All Atoms.

contributes the most to the Hirshfeld surface at 69.5% (Figure 8b). The H−−−S/S−−−H contact contributes 21.6%, resulting in two wings on the side of the fingerprint plot on the Hirshfeld surface (Figure 8c). Other interatomic contacts have relatively small contributions in crystal packing, namely N−−−H/H−−−N and S−−−H/H−−−S, with percentages of 4.8% and 4.1%, respectively.

The interaction of all the atoms inside the Hirshfeld surface with the atoms around the Hirshfeld surface is shown in Figure 9. The exploratory results show that all the atoms inside the Hirshfeld surface interact strongly with the H atoms around the Hirshfeld surface, with a percentage of 86.80%. Similar interactions occur for ALL−S, ALL−N, and ALL−C with contribution percentages of 8.80%, 2.40% and 2.00%, respectively. In the interaction of atoms inside the Hirshfeld surface with atoms around the Hirshfeld surface, the interaction of H atoms with all atoms around the Hirshfeld surface has the most significant contribution of 82.7%. Other interactions are ALL−S, ALL−N, and ALL−C at 12.80%, 2.40% and 2.10%, respectively.

4. CONCLUSION

Tetrakis(N,N'-dietiltiourea)-bis(isothiocyanato)-nickel compound or $[Ni(detu)_4(NCS)_2]$ (denoted as UMCCC-1) has been successfully synthesized using reflux method with acetone and methanol solvents. Single crystals of UMCC-1 in acetone and methanol solvents are dark green in color with melting point 135-137°C and conductivity 66.4-84.4 μS. FTIR absorption band analysis of both crystals is very similar, namely ν(C=S) detu 590 cm^{-1} and,

ν(C≡N) isotiosianato 2119 cm^{-1}. The refinement results show that the two dark green crystals are molecular complexes that have a distorted octahedral geometry with a monoclinic crystal lattice, space group P21/c1 (no.14), crystal lattice parameters a= 11.112(3) Å, b= 17.249(5) Å, c= 9.647(3) Å, and β= 100.785(10). The complex in acetone solvent has better refinement quality than methanol referring to the %R=3.27 and %R=4.55 values, respectively. The crystalline UMCC-1 shows intermolecular N−H−−−S(isothiocyanato) hydrogen bonds and intramolecular N−H−−−S(detu) hydrogen bonds with Hirshfeld surface analysis showing a significant contribution of H−−−H (69.5%).

5. ACKNOWLEDGEMENT

All authors would like to thank Universitas Negeri Malang for supporting this research under the PNBP grant (5.4.520/UN32.20.1 /LT/2023 as bachelor thesis grant) and partially supporting RKI grant (10.5.72/UN32.20.1/LT/2023). This work was also supported by the Center of Advanced Materials for Renewable Energy (CAMRY) laboratory, Universitas Negeri Malang. The Single X-ray Diffraction of complexes was collected in the UM Integrated laboratory, Universitas Negeri Malang (UM), Indonesia.

REFERENCES

Ahghari, M. R., V. Soltaninejad, and A. Maleki (2020). Synthesis of Nickel Nanoparticles by a Green and Convenient Method As a Magnetic Mirror with Antibacterial Activities. *Scientific Reports*, **10**(1); 12627

Ahmad, S., Q. Amir, G. Naz, A. Fazal, M. Fettouhi, A. A. Isab, T. Rüffer, and H. Lang (2012). Synthesis and Crystal Structures of Cadmium Iodide Complexes of N,N'-Diethylthiourea and 1,3-Diazinane-2-thione. *Journal of Chemical Crystallography*, **42**; 615–620

Ahmad, S., M. Fettouhi, T. Roisnel, M. A. Alotaibi, A. I. Alharthi, M. R. Malik, I. Ahmad, and A. A. Isab (2017). Structural Diversity in Pseudohalide Complexes of Cadmium(II) with N-Methylthiourea (Metu): Polymeric $[Cd(Metu)_2(NCS)_2]_n$ Versus Monomeric $[Cd(Metu)_2(CN)_2]$. *Journal of Coordination Chemistry*, **70**(21); 3692–3701

Ajibade, P. A., N. H. Zulu, and A. O. Oyedeji (2013). Synthesis, Characterization, and Antibacterial Studies of Some Metal Complexes of Dialkyl Thiourea: The X-Ray Single Crystal Structure of $[CoCl_2(detu)_2]$. *Synthesis and Reactivity in Inorganic, Metal-Organic, and Nano-Metal Chemistry*, **43**(5); 524–531

Al-Hazmi, G. A. and N. El-Metwally (2017). A Series of Nickel(II) Complexes Derived from Hydrazide Derivatives, Electrochemical, Thermal and Spectral Studies. *Arabian Journal of Chemistry*, **10**; S1003–S1013

Al-Omair, M. A., A. Touny, and M. Saleh (2017). Reflux-Based Synthesis and Electrocatalytic Characteristics of Nickel Phosphate Nanoparticles. *Journal of Power Sources*, **342**; 1032–1039

Alekseeva, E. V., I. A. Chepurnaya, V. V. Malev, A. M. Timonov, and O. V. Levin (2017). Polymeric Nickel Complexes with Salen-Type Ligands for Modification of Supercapacitor Electrodes: Impedance Studies of Charge Transfer and Storage Properties. *Electrochimica Acta*, **225**; 378–391

Alfurayj, I. A., V. G. Young Jr, and M. P. Jensen (2016). Structural Characterization of Thermochromic and Spin Equilibria in Solid-State $Ni(detu)_4Cl_2$ (detu= N,N'-Diethylthiourea). *Inorganic Chemistry*, **55**(4); 1469–1479

Ashfaq, M., K. S. Munawar, M. N. Tahir, N. Dege, M. Yaman, S. Muhammad, S. S. Alarfaji, H. Kargar, and M. U. Arshad (2021). Synthesis, Crystal Structure, Hirshfeld Surface Analysis, and Computational Study of a Novel Organic Salt Obtained from Benzylamine and an Acidic Component. *ACS Omega*, **6**(34); 22357–22366

Asif, I., M. N. Arshad, A. M. Asiri, W. Zierkiewicz, M. Malik-Gajewska, M. I. Mukhtar, M. Mateen, A. A. Isab, and S. Ahmad (2019). Synthesis and Molecular Structure of Polymeric bis(N-methylthiourea-κS)bis(thiocyanato-κN)nickel(II), $[Ni(Metu)_2(NCS)_2]_n$; DFT Analysis of $[Ni(Metu)_2(NCS)_2]_n$ and $[Ni(Thiourea)_2\ (NCS)_2]_n$. *Journal of Molecular Structure*, **1189**; 66–72

Aziz, I., M. Sirajuddin, A. Munir, S. Tirmizi, S. Nadeem, M. Tahir, and W. Sajjad (2018). Synthesis, Characterization, DNA Interaction Study, Antibacterial and Anticancer Activities of New Palladium(II) Phosphine Complexes. *Russian Journal of General Chemistry*, **88**; 551–559

Azouzi, K., B. Hamdi, R. Zouari, and A. B. Salah (2017). Synthesis, Structure and Hirshfeld Surface Analysis, Vibrational and DFT Investigation of (4-Pyridine Carboxylic Acid) Tetrachlorocuprate(II) Monohydrate. *Bulletin of Materials Science*, **40**; 289–299

Banerjee, S., B. Wu, P.-G. Lassahn, C. Janiak, and A. Ghosh (2005). Synthesis, Structure and Bonding of Cadmium(II) Thiocyanate Systems Featuring Nitrogen Based Ligands of Different Denticity. *Inorganica Chimica Acta*, **358**(3); 535–544

Barma, A., M. Chakraborty, S. K. Bhattacharya, P. Ghosh, and P. Roy (2022). Mononuclear Nickel(II) Complexes As Electrocatalysts in Hydrogen Evolution Reactions: Effects of Alkyl Side Chain Lengths. *Materials Advances*, **3**(20); 7655–7666

Baydere, C., M. Taşçı, N. Dege, M. Arslan, Y. Atalay, and I. A. Golenya (2019). Crystal Structure and Hirshfeld Surface Analysis of (E)-2-(2,4,6-trimethylbenzylidene)-3,4-dihydronaphthalen-1(2H)-one. *Acta Crystallographica Section E: Crystallographic Communications*, **75**(6); 746–750

Bhola, Y. O., B. N. Socha, S. B. Pandya, R. P. Dubey, and M. K. Patel (2019). Molecular Structure, DFT Studies, Hirshfeld Surface Analysis, Energy Frameworks, and Molecular Docking Studies of Novel (E)-1-(4-chlorophenyl)-5-methyl-N'-((3-methyl-5-phenoxy-1-phenyl-1H-pyrazol-4-yl) methylene)-1H-1, 2, 3-triazole-4-carbohydrazide. *Molecular Crystals and Liquid Crystals*, **692**(1); 83–93

Binzet, G., G. Kavak, N. Külcü, S. Özbey, U. Flörke, H. Arslan (2013). Synthesis and Characterization of Novel Thiourea Derivatives and Their Nickel and Copper Complexes. *Journal of Chemistry*, **2013**

Bowmaker, G. A., C. Pakawatchai, S. Saithong, B. W. Skelton, and

A. H. White (2009). 1:1 Complexes of Silver(I) Thiocyanate with (Substituted) Thiourea Ligands. *Dalton Transactions*, (14); 2588–2598

Breitenfeld, J., R. Scopelliti, and X. Hu (2012). Synthesis, Reactivity, and Catalytic Application of a Nickel Pincer Hydride Complex. *Organometallics*, **31**(6); 2128–2136

Craig, G. A., A. Sarkar, C. H. Woodall, M. A. Hay, K. E. Marriott, K. V. Kamenev, S. A. Moggach, E. K. Brechin, S. Parsons, and G. Rajaraman (2018). Probing the Origin of the Giant Magnetic Anisotropy in Trigonal Bipyramidal Ni(II) under High Pressure. *Chemical Science*, **9**(6); 1551–1559

Danchovski, Y., H. Rasheev, R. Stoyanova, and A. Tadjer (2022). Molecular Engineering of Quinone-Based Nickel Complexes and Polymers for All-Organic Li-Ion Batteries. *Molecules*, **27**(20); 6805

Feddaoui, I., M. S. Abdelbaky, S. García-Granda, K. Essalah, C. B. Nasr, and M. Mrad (2019). Synthesis, Crystal Structure, Vibrational Spectroscopy, DFT, Optical Study and Thermal Analysis of a New Stannate(IV) Complex Based on 2-ethyl-6-methylanilinium $(C_9H_{14}N)_2$ $[SnCl_6]$. *Journal of Molecular Structure*, **1186**; 31–38

Galet, A., M. C. Muñoz, A. B. Gaspar, and J. A. Real (2005). Architectural Isomerism in the Three-Dimensional Polymeric Spin Crossover System $Fe(pmd)_2[Ag(CN)_2]_2$: Synthesis, Structure, Magnetic Properties, and Calorimetric Studies. *Inorganic Chemistry*, **44**(24); 8749–8755

Hannachi, A., A. Valkonen, M. Rzaigui, and W. Smirani (2019). Thiocyanate Precursor Impact on the Formation of Cobalt Complexes: Synthesis and Characterization. *Polyhedron*, **161**; 222–230

Monim-ul Mehboob, M., M. Akkurt, I. U. Khan, S. Sharif, I. Asif, and S. Ahmad (2010). Hexakis(thiourea-κS) Nickel(II) Nitrate: A Redetermination. *Acta Crystallographica Section E: Structure Reports Online*, **66**(8); i57–i58

Mufakkar, M., A. A. Isab, T. Rüffer, H. Lang, S. Ahmad, N. Arshad, and A. Waheed (2011). Synthesis, Characterization, and Antibacterial Activities of Copper(I) Bromide Complexes of Thioureas: X-Ray Structure of $[Cu(Metu)_4]Br$. *Transition Metal Chemistry*, **36**; 505–512

Nadeem, S., M. K. Rauf, S. Ahmad, M. Ebihara, S. A. Tirmizi, S. A. Bashir, and A. Badshah (2009). Synthesis and Characterization of Palladium(II) Complexes of Thioureas. X-Ray Structures of $[Pd(N,N'-dimethylthiourea)_4]Cl_2 \cdot 2H_2O$ and $[Pd(tetramethylthiourea)_4]Cl_2$. *Transition Metal Chemistry*, **34**; 197–202

Nardelli, M., G. F. Gasparri, A. Musatti, and A. Manfredotti (1966). The Crystal and Molecular Structure of bis-(2-thioimidazolidine)-nickel(II) Thiocyanate. *Acta Crystallographica*, **21**(6); 910–919

Neumann, T., M. Ceglarska, L. S. Germann, M. Rams, R. E. Dinnebier, S. Suckert, I. Jess, and C. Näther (2018). Structures, Thermodynamic Relations, and Magnetism of Stable and Metastable $Ni(NCS)_2$ Coordination Polymers. *Inorganic Chemistry*, **57**(6); 3305–3314

Psycharis, V., D. Dermitzaki, and C. P. Raptopoulou (2021). The Use of Hirshfeld Surface Analysis Tools to Study the Intermolecular Interactions in Single Molecule Magnets. *Crystals*, **11**(10); 1246

Sugiyama, H., A. Sekine, and H. Uekusa (2015). Crystal Structure of Bis(4-aminopyridine)bis(isothiocyanato)cobalt(II). *X-Ray Structure Analysis Online*, **31**; 27–28

Tabatabaee, M. and S. Saheli (2011). Synthesis, Structural and Thermal Studies of a New Nickel Complex Containing 2-Aminopyrimidine and Thiocyanate Mixed Ligands with a Three-Dimensional Network Structure. *Journal of Chemical Crystallography*, **41**; 670–673

Tanase, S., M. Ferbinteanu, M. Andruh, C. Mathonière, I. Strenger, and G. Rombaut (2000). Synthesis and Characterization of a New Molecular Magnet,$[Ni(ampy)_2]_3[Fe(CN)_6]_2 \cdot 6H_2O$, and Synthesis, Crystal Structure and Magnetic Properties of its Mononuclear Precursor, Trans-$[Ni(ampy)_2(NO_3)_2]$(ampy=2-Aminomethylpyridine). *Polyhedron*, **19**(16-17); 1967–1973

Tsague Chimaine, F., D. M. Yufanyi, A. Colette Benedicta Yuoh, D. B. Eni, and M. O. Agwara (2016). Synthesis, Crystal Structure, Photoluminescent and Antimicrobial Properties of a Thiocyanato-Bridged Copper(II) Coordination Polymer. *Cogent Chemistry*, **2**(1); 1253905

Wada, A., Y. Honda, S. Yamaguchi, S. Nagatomo, T. Kitagawa, K. Jitsukawa, and H. Masuda (2004). Steric and Hydrogen-Bonding Effects on the Stability of Copper Complexes with Small Molecules. *Inorganic Chemistry*, **43**(18); 5725–5735

Wahyuni, R. M., H. W. Wijaya, M. E. F. Sari, I. W. Dasna, and N. Farida (2022). Synthesis and Characterization of Complex Compounds from Cadmium(II)Chloride and Cobalt(II)Chloride with N,N'-Diethylthiourea. *Journal of Pure & Applied Chemistry Research*, **11**(1); 1–8

Yufanyi, D. M., H. J. Nono, A. C. B. Yuoh, C. D. Tabong, W. Judith, and A. M. Ondoh (2021). Crystal Packing Studies, Thermal Properties and Hirshfeld Surface Analysis in the Zn(II) Complex of 3-Aminopyridine with Thiocyanate As Co-Ligand. *Open Journal of Inorganic Chemistry*, **11**(3); 63–84

Zhang, Z., J. Xu, S. Yan, Y. Chen, Y. Wang, Z. Chen, and C. Ni (2017). Two Organic Cation Salts Containing Tetra (isothiocyanate) Cobaltate (ii): Synthesis, Crystal Structures, Spectroscopic, Optical and Magnetic Properties. *Crystals*, **7**(3); 92

